Journal of Hazardous Materials 185 (2011) 408–415

Contents lists available at ScienceDirect

Journal of Hazardous Materials

journal homepage: www.elsevier.com/locate/jhazmat

# On the zinc sorption by the Serbian natural clinoptilolite and the disinfecting ability and phosphate affinity of the exhausted sorbent

Djordje Stojakovic[a], Jasna Hrenovic[b], Matjaz Mazaj[c], Nevenka Rajic[d,*]

[a] Innovation Centre of the Faculty of Technology and Metallurgy, University of Belgrade, 11000 Belgrade, Serbia
[b] Faculty of Science, University of Zagreb, Roosveltov trg 6, 10000 Zagreb, Croatia
[c] National Institute of Chemistry, Hajdrihova 19, 1000 Ljubljana, Slovenia
[d] Faculty of Technology and Metallurgy, University of Belgrade, 11000 Belgrade, Serbia

ARTICLE INFO

*Article history:*
Received 16 June 2010
Received in revised form
14 September 2010
Accepted 15 September 2010
Available online 22 September 2010

*Keywords:*
Zinc removal
Kinetics
Antibacterial activity
Phosphate removal
Nano-ZnO

ABSTRACT

The Serbian natural zeolite is moderately effective in removing the zinc(II) ions from aqueous solutions. At 298 K the sorption capacity varies from 13 to 26% for the initial Zn(II) solution concentration of 100 and 600 mg Zn $dm^{-3}$, respectively. The sorption isotherm at 298–338 K is best represented by the Langmuir model and the sorption kinetics by the pseudo-second-order model. The sorption involves a combination of film diffusion, intra-particle diffusion, and a chemical cation-exchange between the $Na^+$ ions of clinoptilolite and $Zn^{2+}$ ions. The sorption was found to be endothermic and spontaneous in the 298–338 K range. The exhausted sorbent can remove phosphate ions and it exhibits an excellent antibacterial activity towards *Acinetobacter junii*. By dehydration at about 500 °C it transforms to a ZnO-containing product featuring nano-sized wurtzite ZnO particles widespread over the clinoptilolite surface.



## 1. Introduction

Release of toxic heavy metals into environment can cause serious soil and water pollution. Industrial wastewaters often have a considerable content of heavy metal ions which necessitates that such waters be appropriately treated prior to their discharge. Due to their adsorbent, ion-exchange and catalytic properties, zeolitic materials attract a great attention. Adsorption using natural adsorbents is generally considered to be the most suitable method for wastewater treatment. Clinoptilolite, as the most abundant natural zeolite, can therefore be regarded as a cost minimizing choice of the adsorbent for the developing countries.

Recently a detailed spectroscopic and structural investigation of the zinc loaded natural zeolitic tuff from south Serbia region (Zlatokop mine) has been reported [1]. It was found that the zeolitic tuff contains three major mineral phases, the clinoptilolite being in the highest percentage (more than 70 wt.%). Treatment of the zeolite with aqueous zinc(II) solutions yielded zinc-loaded samples with the zinc ions being present exclusively in the clinoptilolite lattice [1]. Therefore the zeolitic tuff could be suitable as sorbent in removing the $Zn^{2+}$ ions from wastewaters.

In this paper we report in detail on the kinetic, thermodynamic and some biological aspects of the $Zn^{2+}$ sorption by clinoptilolite at different temperatures and different $Zn^{2+}$ solution concentrations. One aim of the study is to obtain parameters for a subsequent design of a pilot installation for the $Zn^{2+}$ removal from wastewater. Secondly, since zinc is among the metals which exhibit antibacterial properties [2], we have also investigated the zinc-containing clinoptilolite as an antibacterial material, having in mind a possible utilization of the sludge. Millions of tons of residual sludge come out of the wastewater treatment plants annually. Management of the sludge is a major part of the waste treatment since up to 60% of the total cost of operating and maintaining wastewater treatment plants is related to sludge management [3]. For this reason, various methods have been proposed [4] with the aim of minimizing possible health risks of sludge disposal.

## 2. Experimental

### 2.1. Zn sorption on the clinoptilolite tuff

The zeolite material (CLI) obtained from a large sedimentary Zlatokop deposit was used in the experiments. The particle size of the samples was in the range of 0.063–0.1 mm. The sample (1.000 g) was pretreated with 100.00 $cm^3$ of 2.0 mol $dm^{-3}$ solution of NaCl (p.a., Aldrich) in order to improve the tuff's exchange capacity [1,5].

* Corresponding author. Fax: +381 11 3370 387.
*E-mail address:* nena@tmf.bg.ac.rs (N. Rajic).

0304-3894/$ – see front matter © 2010 Published by Elsevier B.V.
doi:10.1016/j.jhazmat.2010.09.048

The suspension was magnetically stirred for 24 h at 25 °C. The sample (Na-CLI) was then washed by distilled water and dried in oven at 105 °C. Elemental analysis showed [1] that the amount of exchangeable cations in Na-CLI theoretically allows for an uptake (by cation exchange) of approx. 40 mg Zn per gram of Na-CLI.

The Zn(II) sorption isotherms were determined at 298, 308, 318, 328 and 338 K using the batch method. 1.000 g of the Na-CLI was placed in 100.00 $cm^3$ of the $ZnCl_2$ (p.a., Aldrich) solution of chosen concentration. The Zn(II) concentrations were 100, 200, 300, 400 and 600 mg Zn $dm^{-3}$. The suspension was shaken at about 100 rpm for 24 h in a thermostated water bath (Memmert WPE 45). The solid, Zn-loaded Na-CLI (Zn-CLI), was then recovered by filtration.

The rate of sorption of Zn(II) by Na-CLI was studied at temperatures of 298, 308, 318 and 328 K in solutions with an initial $ZnCl_2$ concentration of 100, 200, 300 and 400 mg Zn $dm^{-3}$. 100.00 $cm^3$ of the solution was mixed with 1.0 g of Na-CLI and the suspension was shaken at a rate of about 100 rpm for a time period from 20 min to 24 h. The solid was then separated by filtration.

Preliminary investigations showed that the $Zn^{2+}$ removal capacity of Na-CLI increases slightly when the solution pH is raised from 4 to 7. The subsequent experiments were conducted at pH about 6 to avoid any possible hydroxide precipitation [6]

Zinc concentrations in solution were determined by AAS using Varian Spectra AA 200; at least five measurements were done for each determination. The X-ray Photoelectron Spectroscopy (XPS or ESCA) analysis was carried out on the PHI-TFA XPS spectrometer, exciting the sample surface by X-ray radiation from an Al anode. The samples were in the form of 1 mm thick pressed pellets. The procedure details were reported previously [5].

All the experiments were carried out under controlled conditions: the temperature in the thermostated bath was maintained constant to within ±0.1 °C, the clinoptilolite sample was weighted to four-digit accuracy, and the solution concentrations were determined with four-digit accuracy.

### 2.2. Thermal analysis and thermal treatment of Zn-CLI

Thermal analysis of Zn-CLI was performed using a SDT Q-600 simultaneous DSC-TGA instrument (TA Instruments). The sample (mass approx. 10 mg) was heated in a standard alumina sample pan, the experiment being carried out under air with a flow rate of 0.1 $dm^3$ $min^{-1}$.

The sample of Zn-CLI (containing 8.8 mg Zn $g^{-1}$) was thermally treated under air at 540 °C at a heating rate of 10 °C $min^{-1}$. The obtained orange-colored product (ZnO-CLI) was analyzed by the transmission electron microscopy (TEM). The procedure details were reported previously [7]. Identification of the crystal phase formed during the thermal treatment of Zn-CLI was done using the selected area electron diffraction (SAED) over multiple nanocrystals.

### 2.3. Antibacterial activity analysis

A pure culture of *Acinetobacter junii* DSM 1532 has been used for testing the antibacterial activity of Zn-containing samples (Zn-CLI and ZnO-CLI). This bacterium was used here in the bioassay and is not specifically related to the estimation of wastewater toxicity. This Gram-negative bacterium is normally present in wastewater and in the activated sludge biomass. The most widely studied physiological characteristic of this bacterium is its ability to accumulate the soluble phosphate present in wastewater in the form of intracellular insoluble polyphosphate granules [8].

The *A. junii* was pregrown on the nutrient agar (Biolife, Italy) for 16 h at 30.0 ± 0.1 °C. Next, the biomass was suspended (using a mechanical shaker Kartell TK3S) in sterile 0.05 mol $dm^{-3}$ NaCl and inoculated into 100 $cm^3$ of autoclaved synthetic wastewater (composition in mg $dm^{-3}$ of distilled water: Na-propionate 300; peptone 100; $MgSO_4 \cdot 7H_2O$ 10; $CaCl_2 \cdot 2H_2O$ 6; KCl 30; yeast extract 20; $KH_2PO_4$ 88; pH = 7.0 ± 0.2). 1.00 g of Zn-CLI (or ZnO-CLI) was added into the flask, while a control flask was left without addition of the material. The flasks were sealed with a sterile gum cap having a central hole through which aeration with filtered air (1 $dm^3$ $min^{-1}$) was provided. The flasks were incubated for 24 h at 30.0 ± 0.5 °C in a water bath (Memmert WNB22) with stirring (70 rpm).

All analytical measurements were carried out in triplicate. The pH-value was measured with WTW 330 pH-meter. The concentration of phosphorous in wastewater was measured (after filtration through Whatman filter units of pore diameter 0.2 μm) in a DR/2500 Hach spectrophotometer by the molybdovanadate method (Hach method 8114). The number of viable bacterial cells (either planktonic or immobilized onto material) was determined as colony-forming units (CFU) grown on the nutrient agar after incubation at 30 ± 0.1 °C for 24 h. For the determination of planktonic bacteria, 1 $cm^3$ of supernatant was serially diluted ($10^{-1}$–$10^{-9}$) and volumes of 0.1 $cm^3$ were aseptically inoculated onto nutrient agar (spread plate method). After incubation, the bacterial colonies were counted and the number of viable cells was reported as CFU $dm^{-3}$. In order to determine the number of immobilized cells, the material was taken from the flask, washed three times with sterile 0.05 mol $dm^{-3}$ NaCl solution, and aseptically placed into a tube containing 9 $cm^3$ of 0.05 mol $dm^{-3}$ NaCl. The sample was crushed with a sterile glass rod and vigorously shaken on a mechanical shaker (40 Hz/3 min, Kartell TK3S). This procedure [9] detaches immobilized cells from the carrier so that they remain in the suspension. From such suspension, serial dilutions were made and nutrient agar plates were inoculated and incubated as already described. After the incubation the colonies were counted and the remaining carrier samples were dried and weighted. The number of cells was reported as immobilized CFUs per one gram of the dry carrier. Statistica Software 8.0 (StatSoft, Tulsa, USA) was used for statistical analysis. The numbers of bacterial CFU were logarithmically transformed beforehand to normalize distribution and to equalize variances of the measured parameters. The comparisons between the samples were done using the one-way analysis of variance (ANOVA), and subsequently the post hoc Duncan test was performed for the calculations concerning pairwise comparisons. Statistical decisions were made at a significance level of $p < 0.05$.

### 2.4. Leaching test

1.00 g of Zn-CLI was suspended into 100.00 $cm^3$ of synthetic wastewater (pH adjusted to 7) and left for 24 h in a thermostated water bath at 30 °C. After filtration the Zn content in the filtrate was analyzed by AAS.

## 3. Results and discussion

### 3.1. Sorption isotherms

Fig. 1 shows the sorption isotherms for the Zn(II) on clinoptilolite at 298, 308, 318, 328 and 338 K. It is seen that the sorption capacity of the clinoptilolite increases both with temperature and with the initial Zn(II) solution concentration. The clinoptilolite is moderately effective in removing the zinc(II) ions from aqueous solutions at ambient temperature: the sorption capacity at 298 K varies from 5.8 mg Zn $g^{-1}$ (for $C_0$ = 100 mg Zn $dm^{-3}$) to 11.3 mg Zn $g^{-1}$ (for $C_0$ = 600 mg Zn $dm^{-3}$), which corresponds to 13–26% cation exchange. There is a roughly 1.4-fold increase in sorption capacity at 338 K: from 8.2 mg Zn $g^{-1}$ (for $C_0$ = 100 mg Zn $dm^{-3}$) to

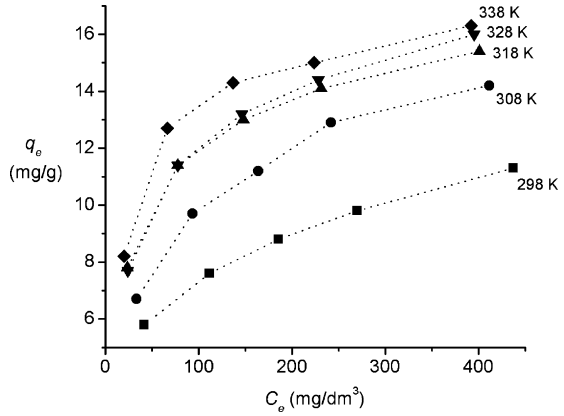


**Fig. 1.** The sorption isotherms for Zn(II) on Na-CLI; $q_e$ is the amount of the sorbed metal (mg per 1 g of Na-CLI) and $C_e$ is the solution concentration at equilibrium.

16.3 mg Zn $g^{-1}$ (for $C_0$ = 600 mg Zn $dm^{-3}$), corresponding to 18–37% cation exchange.

The equilibrium data from Fig. 1 have been analyzed by several empirical adsorption isotherm models [10]. Among the two-parameter models only the Langmuir model [11] gave fits that are acceptable both mathematically and physicochemically. Similar conclusions were reported for the $Zn^{2+}$ sorption by natural clinoptilolites from other sources [12], as well as by some other sorbents [13,14]. Among the three-parameter models, the Langmuir–Freundlich or Sips model [11] gave fits that are mathematically satisfactory; however, the fits are not acceptable from the physicochemical point of view (*vide infra*).

The Langmuir model can be represented as:

$$q_e = \frac{q_{max} b_L C_e}{1 + b_L C_e} \quad (1)$$

where $C_e$ is the equilibrium concentration of the solute (mg $dm^{-3}$), $q_e$ is the equilibrium concentration of the solute adsorbed (mg $g^{-1}$), while $q_{max}$ (mg $g^{-1}$) and $b_L$ ($dm^3$ $mg^{-1}$) are Langmuir constants ($q_{max}$ corresponding to the maximum achievable uptake by a system, and $b_L$ is related to the affinity between the sorbate and the sorbent).

The Langmuir–Freundlich model was applied in the Sips form [11]:

$$q_e = \frac{q_{max} (b_S C_e)^{n_S}}{1 + (b_S C_e)^{n_S}} \quad (2)$$

where $b_S$ is the Sips isotherm constant and $n_S$ is the Sips model exponent.

The analysis of the isotherm data using Eqs. (1) and (2) gave parameters listed in Table 1. In mathematical sense (i.e. judging by the $R^2$ values), the Sips model gives somewhat better fits (probably because it uses three adjustable parameters, while the Langmuir model uses only two). However, from the physicochemical point of view only the Langmuir isotherm gives a realistic description of the studied adsorption. Two facts in Table 1 suggest such a conclusion. Firstly, the $q_{max}$ values obtained by the Langmuir fits are very close to the experimentally measured values, whereas those obtained by the Sips model are quite larger (especially for the temperature of 298 K). Secondly, while the Langmuir fits show that $q_{max}$ increases with increasing temperature, i.e. the same trend as experimentally observed (Fig. 1), the $q_{max}$ values obtained by the Sips model do not show such behavior.

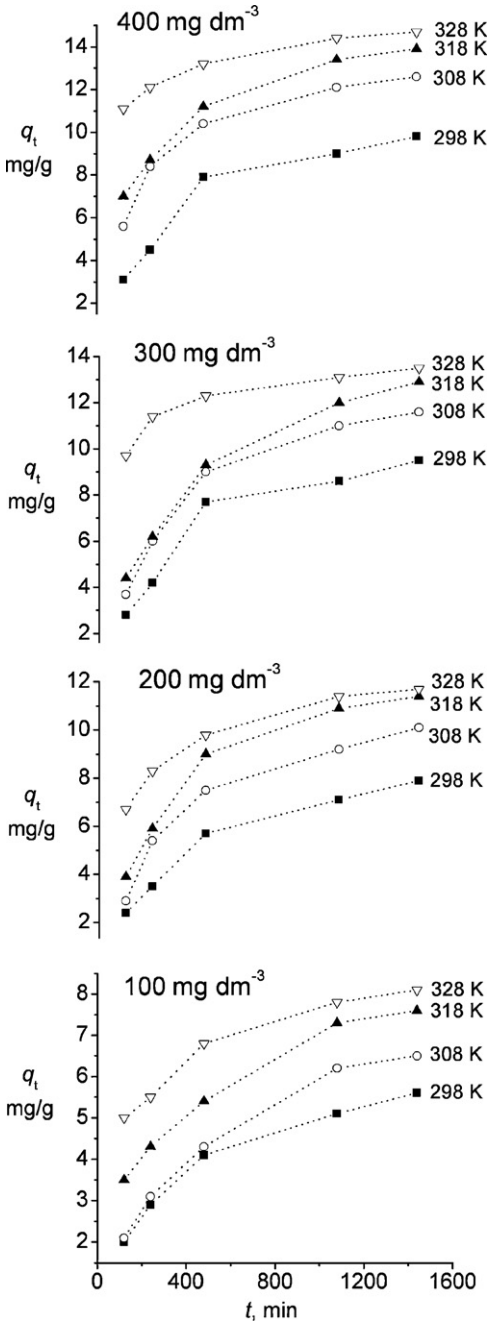


**Fig. 2.** Sorption kinetics for Zn(II) on Na-CLI for different initial Zn(II) concentrations; $q_t$ is the amount of the sorbed Zn(II) (mg per 1 g of Na-CLI) after time $t$.

### 3.2. Kinetic analysis

The Zn(II) sorption dependence on time was investigated at 298, 308, 318 and 328 K for solutions with $C_0$ = 100, 200, 300 and 400 mg Zn $dm^{-3}$. The time dependence was followed until the sorption equilibrium has essentially been reached, the latter occurring in about 24 h. Fig. 2 shows the uptake values of Zn(II) from solution.

It is seen from the curves on Fig. 2 that at the beginning stages of sorption (i.e. approximately in the first 100–120 min), the Zn(II) uptake increases rather sharply from $q_t$ = 0 at $t$ = 0; this sharp step is particularly evident for temperatures of 308 K and above. Afterwards the sorption proceeds more gradually. Similar behavior has been reported for the $Zn^{2+}$ sorption by other sorbents [14,15]. The data from Fig. 2 were analyzed using two reaction-based kinetic models and a diffusion-based model.

**Table 1**
Parameters obtained by the adsorption isotherm Eqs. (1) and (2) for the sorption of Zn(II) on Na-CLI; $R^2$ is the correlation coefficient.

| $T$ (K) | Sips isotherm | | | | Langmuir isotherm | | |
|---|---|---|---|---|---|---|---|
| | $q_{max}$ (mg g$^{-1}$) | $b_S$ (dm$^3$ mg$^{-1}$) | $n_S$ | $R^2$ | $q_{max}$ (mg g$^{-1}$) | $b_L$ (dm$^3$ mg$^{-1}$) | $R^2$ |
| 298 | 170 | $3.41 \times 10^{-7}$ | 0.301 | 0.999 | 12.0 | 0.0184 | 0.930 |
| 308 | 22.6 | 0.00636 | 0.560 | 0.996 | 15.5 | 0.0198 | 0.971 |
| 318 | 19.5 | 0.0221 | 0.603 | 0.999 | 15.8 | 0.0373 | 0.977 |
| 328 | 21.7 | 0.0150 | 0.576 | 0.999 | 16.6 | 0.0319 | 0.974 |
| 338 | 17.5 | 0.0441 | 0.857 | 0.995 | 16.8 | 0.0468 | 0.992 |

The first reaction-based model is described by the Lagergren's first-order rate expression ("pseudo-first-order rate equation") [16]; its integrated form is given by Eq. (3):

$$\log(q_e - q_t) = \log q_e - \frac{k_1}{2.203} t \quad (3)$$

where $q_e$ (mg g$^{-1}$) is the adsorption capacity at equilibrium and $k_1$ (min$^{-1}$) is the rate constant of the first-order adsorption. When the experimental data agree with this model, the plot of $\log(q_e - q_t)$ vs. $t$ yields a straight line.

The second reaction-based model is defined [16] by the pseudo-second-order rate equation which has the following integrated form:

$$\frac{t}{q_t} = \frac{1}{k_2 q_e^2} + \frac{1}{q_e} t \quad (4)$$

where $k_2$ (g mg$^{-1}$ min$^{-1}$) is the rate constant of the pseudo-second-order adsorption. The plot of $t/q_t$ vs. $t$ is a straight line if the experimental data correspond to this model; $q_e$ and $k_2$ are obtained from the slope and intercept, respectively.

Application of the two models showed that the pseudo-second-order model gives a slightly better description of the Zn(II) sorption kinetics as judged by the $R^2$ values (Table 2). This agrees with general observations in heavy metal sorption studies [13,15,17,18].

The results in Table 2 show that the $k_1$ and $k_2$ rate constant values obtained for the two models change rather irregularly with temperature for all initial Zn(II) concentrations. At least two factors could be responsible for that. Firstly, even though the spectroscopic analyses confirm that the zinc(II) removal by clinoptilolite occurs via ion exchange [1], the ion-exchange reaction might not alone be adequate in explaining the sorption kinetics of $Zn^{2+}$; diffusional processes have also to be taken into account. Secondly, the species entering the clinoptilolite lattice need not be only the hydrated $Zn^{2+}$ ions but also some more complex zinc(II) ionic moieties. Namely, it has been well known that in aqueous solution of zinc salts hydrolysis is quite common, the hydrolysis degree increasing with temperature. The presence of such hydrolysis is indirectly supported by spectroscopic analysis (Fig. 3) which shows that the zinc concentration decreases slightly from the surface to the interior of the clinoptilolite particles. The bulkiness of the hydrolysis products could be the reason for such a concentration decrease. (Fig. 3 in addition confirms that Na-CLI has a better zinc removal efficiency than the original CLI.)

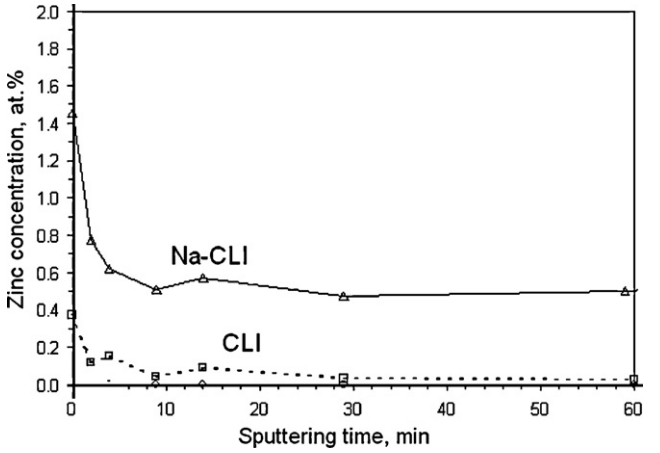


**Fig. 3.** In-depth dependance of the Zn concentration obtained by XPS depth profiling as a function of the sputtering time on the zinc-loaded samples. Na-CLI: Zn-containing sample obtained from Na-CLI; CLI: Zn-containing sample obtained from CLI. The estimated analyzed depth is about 60 nm.

**Table 2**
Rate constants for the three studied kinetic models for the sorption of Zn(II) on Na-CLI ($R$ is the correlation coefficient of the linear regression).

| $C_0$ (mg Zn dm$^{-3}$) | $T$ (K) | Weber–Morris model parameters[a] | | | Lagergren's first-order rate constants | | Pseudo-second-order rate parameters | | |
|---|---|---|---|---|---|---|---|---|---|
| | | $k_d$ (mg g$^{-1}$ min$^{-1/2}$) | $I$ (mg g$^{-1}$) | $R^2$ | $k_1$ (min$^{-1}$) | $R^2$ | $k_2$ (g mg$^{-1}$ min$^{-1}$) | $q_e$ (mg g$^{-1}$) | $R^2$ |
| 100 | 298 | 0.0932 | 2.05 | 0.999 | $2.04 \times 10^{-3}$ | 0.995 | $5.00 \times 10^{-4}$ | 6.67 | 0.998 |
| | 308 | 0.0590 | 4.26 | 0.999 | $2.83 \times 10^{-3}$ | 0.985 | $3.06 \times 10^{-4}$ | 8.30 | 0.996 |
| | 318 | 0.0590 | 5.36 | 0.999 | $2.76 \times 10^{-3}$ | 0.980 | $4.77 \times 10^{-4}$ | 8.81 | 0.994 |
| | 328 | 0.0827 | 5.01 | 0.991 | $2.49 \times 10^{-3}$ | 0.998 | $9.54 \times 10^{-4}$ | 8.71 | 0.999 |
| 200 | 298 | 0.136 | 2.71 | 0.997 | $2.02 \times 10^{-3}$ | 0.987 | $2.50 \times 10^{-4}$ | 9.98 | 0.995 |
| | 308 | 0.161 | 3.96 | 0.999 | $2.09 \times 10^{-3}$ | 0.983 | $2.30 \times 10^{-4}$ | 12.5 | 0.996 |
| | 318 | 0.153 | 5.69 | 0.986 | $2.83 \times 10^{-3}$ | 0.997 | $2.41 \times 10^{-4}$ | 13.87 | 0.998 |
| | 328 | 0.123 | 7.17 | 0.972 | $2.92 \times 10^{-3}$ | 0.998 | $6.44 \times 10^{-4}$ | 12.7 | 0.999 |
| 300 | 298 | 0.107 | 5.23 | 0.957 | $2.10 \times 10^{-3}$ | 0.909 | $2.20 \times 10^{-4}$ | 12.0 | 0.985 |
| | 308 | 0.165 | 5.42 | 0.991 | $2.67 \times 10^{-3}$ | 0.996 | $2.18 \times 10^{-4}$ | 14.3 | 0.998 |
| | 318 | 0.228 | 4.35 | 0.995 | $2.35 \times 10^{-3}$ | 0.994 | $1.83 \times 10^{-4}$ | 15.9 | 0.998 |
| | 328 | 0.0745 | 10.7 | 0.999 | $2.21 \times 10^{-3}$ | 0.969 | $12.5 \times 10^{-4}$ | 13.9 | 0.999 |
| 400 | 298 | 0.116 | 5.33 | 0.986 | $2.23 \times 10^{-3}$ | 0.941 | $2.37 \times 10^{-4}$ | 12.1 | 0.990 |
| | 308 | 0.140 | 7.37 | 0.991 | $2.67 \times 10^{-3}$ | 0.993 | $4.11 \times 10^{-4}$ | 14.1 | 0.999 |
| | 318 | 0.174 | 7.47 | 0.980 | $2.76 \times 10^{-3}$ | 0.996 | $3.77 \times 10^{-4}$ | 15.5 | 0.999 |
| | 328 | 0.0961 | 11.1 | 0.984 | $2.58 \times 10^{-3}$ | 0.999 | $11.1 \times 10^{-4}$ | 15.2 | 0.999 |

[a] The Weber–Morris model parameters refer to the second segment of the $q_t$ vs. $t^{1/2}$ line (see text).

**Table 3**
Thermodynamic parameters for the Zn(II) sorption on Na-CLI ($R$ is the correlation coefficient of the linear regression).

| $C_0$ (mg Zn dm$^{-3}$) | $T$ (K) | $\Delta G^\circ$ (kJ mol$^{-1}$) | $\Delta H^\circ$ (kJ mol$^{-1}$) | $\Delta S^\circ$ (J K$^{-1}$ mol$^{-1}$) | $R^2$ |
|---|---|---|---|---|---|
| 100 | 298 | −14.1 | 22.4 | 123 | 0.915 |
| | 308 | −15.5 | | | |
| | 318 | −17.4 | | | |
| | 328 | −17.8 | | | |
| | 338 | −19.0 | | | |
| 200 | 298 | −12.4 | 20.3 | 110 | 0.931 |
| | 308 | −13.8 | | | |
| | 318 | −15.2 | | | |
| | 328 | −15.7 | | | |
| | 338 | −16.9 | | | |
| 300 | 298 | −11.5 | 15.6 | 91.6 | 0.913 |
| | 308 | −12.8 | | | |
| | 318 | −13.9 | | | |
| | 328 | −14.4 | | | |
| | 338 | −15.2 | | | |
| 400 | 298 | −10.8 | 11.8 | 77.0 | 0.826 |
| | 308 | −12.1 | | | |
| | 318 | −12.9 | | | |
| | 328 | −13.4 | | | |
| | 338 | −14.0 | | | |
| 600 | 298 | −10.0 | 9.49 | 66.0 | 0.855 |
| | 308 | −11.0 | | | |
| | 318 | −11.7 | | | |
| | 328 | −12.2 | | | |
| | 338 | −12.6 | | | |

#### 3.2.1. Diffusion effects

In order to examine the role of diffusion in the sorption process, the data were also analyzed by the Weber–Morris mass transfer model [19]. This model is defined by the rate equation (5):

$$q_t = k_d t^{1/2} + I \tag{5}$$

where $q_t$ (mg g$^{-1}$) is the adsorption capacity at time $t$ (min), $k_d$ (mg g$^{-1}$ min$^{-1/2}$) is the diffusion rate constant and $I$ (mg g$^{-1}$) is the intercept at the ordinate.

The plots of $q_t$ vs. $t^{1/2}$ for various temperatures and various initial Zn(II) concentrations are visually very similar to those shown in Fig. 2 and are not therefore graphically presented. The plots give straight lines consisting of two segments: the first segment occurs in the $t^{1/2}$ region up to about 20 min$^{1/2}$ while the second one corresponds to higher $t^{1/2}$ values. The first segment, with a sharper slope, can be attributed [20] to the diffusion of the $Zn^{2+}$ ions through the solution to the external surface of the adsorbent, i.e. the boundary layer (film) diffusion. The second segment of the lines reflects a gradual adsorption stage, which is characterized by the intraparticle diffusion of $Zn^{2+}$ into clinoptilolite channels and vacancies. Thus there are two diffusional processes that affect the rate of the $Zn^{2+}$ adsorption but only one of them is of importance in a particular time region. The slope of each linear portion indicates the rate of the corresponding adsorption, a lower slope describing a slower adsorption process. Therefore, it follows from the plots that the film diffusion (at the beginning stages) proceeds faster than the intra-particle diffusion (at later stages).

The second segment of the lines in the plots discussed, describing the intraparticle diffusion, has been analyzed by linear regression and the results (included in Table 2) show that in all cases the intercept $I$ is greater than zero. This means [21] that the intra-particle diffusion, although important over longer contact time periods, was not the rate-limiting step in the present study. The intra-particle diffusion can become the rate-limiting step only under vigorous mixing of the suspension [21].

### 3.3. Thermodynamic study

The data obtained by sorption experiments at 298, 308, 318, 328 and 338 K, and the initial Zn(II) concentrations of 100, 200, 300, 400 and 600 mg Zn dm$^{-3}$, were used for the estimation of some thermodynamic parameters. The standard free energy of sorption ($\Delta G^\circ$) was calculated by Eq. (6):

$$\Delta G^\circ = -RT \ln K \tag{6}$$

$R$ is the universal gas constant and $K$ is the equilibrium constant at the temperature $T$. The constant $K$ was calculated as the ratio of the equilibrium Zn(II) concentrations on the sorbent and in solution after 24 h of exchange. The enthalpy and entropy of sorption were calculated from Eq. (7):

$$\ln K = \frac{\Delta S^\circ}{R} - \frac{\Delta H^\circ}{RT} \tag{7}$$

The plot of $\ln K$ vs. $1/T$ gives a straight line (Fig. 4), and the values of $\Delta S^\circ$ and $\Delta H^\circ$ are evaluated from its intercept and slope,

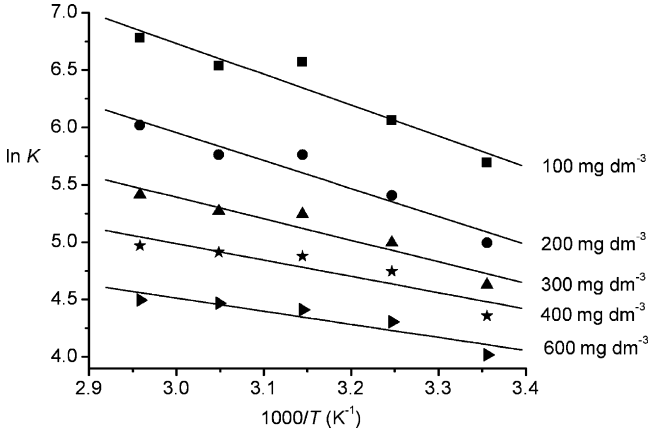


**Fig. 4.** The plot of $\ln K$ ($K$ is the equilibrium constant) vs. $1/T$ for different initial Zn(II) concentrations.

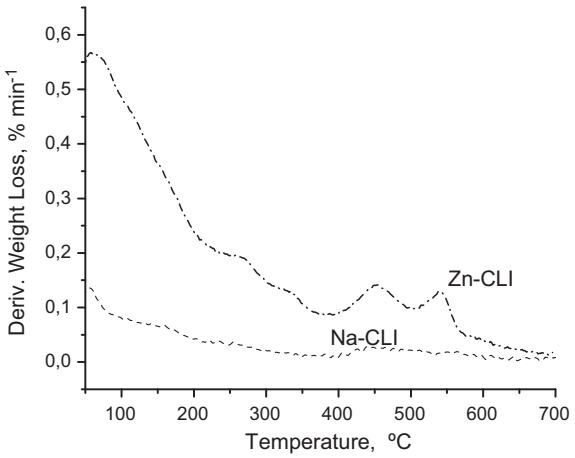


**Fig. 5.** DTG curves of Na-CLI and Zn-CLI.

respectively. The calculated thermodynamic parameters are listed in Table 3.

As can be seen from Fig. 4 and from the $R^2$ values in Table 3, the linearity of the $\ln K$ vs. $1/T$ plot is satisfactory for the initial concentrations of 100, 200 and 300 mg Zn $dm^{-3}$, and less so for 400 and 600 mg Zn $dm^{-3}$.

The $\Delta G^\circ$ values given in Table 3 show that the sorption of Zn(II) on Na-CLI occurs spontaneously in the 298–338 K range. Such spontaneity has also been observed for the sorption of Zn(II) on other zeolites [22]. The spontaneity slightly increases with temperature for all initial Zn(II) concentrations. The Zn(II) sorption is endothermic ($\Delta H^\circ > 0$) and proceeds with an increase in entropy. The positive $\Delta S^\circ$ values reflect the fact that the sorption involves the liberation of two $Na^+$ ions when one $Zn^{2+}$ ion is bound to the sorbent. It is also evident from Table 3 that the spontaneity (at a given temperature), as well as the $\Delta H^\circ$ and $\Delta S^\circ$ values all decrease as the initial Zn(II) concentration increases. It is interesting that the thermodynamic parameters exhibit trends which are partly opposite to those found for the Zn(II) sorption by zeolites NaA and NaX [22]. Namely, in the latter case the Zn(II) sorption is exothermic and proceeds with a decrease of entropy, the spontaneity slightly decreasing with temperature.

### 3.4. Thermal treatment of Zn-CLI

TG and DTG curves of Zn-CLI are very similar to those of Mn-CLI [5]. DTG curves of Na-CLI and Zn-CLI are given in Fig. 5. Similar to the situation found for Mn-CLI, the presence of Zn(II) ions in the CLI framework affects both the water content and the dehydration process. The water content changes from 12 wt.% in Na-CLI to 13 wt.% in Zn-CLI. The dehydration of Na-CLI is rather continuous with only one broad weak maximum at about 450 °C, whereas the DTG curves of both Zn-CLI and Mn-CLI display several maxima indicating a multistep dehydration. The strongest DTG maxima for Zn-CLI are at 450 and 540 °C. The multistep dehydration is probably a consequence of the following process occurring above 400 °C: the zinc ions migrate, gradually losing water molecules from their hydration sphere and form zinc oxide clusters.

TEM analysis confirms that the dehydration of Zn-CLI leads to the formation of zinc oxide and it further shows that the zinc oxide is present in the form of nano particles; the latter are widespread over the clinoptilolite surface (Fig. 6a). The average size of the spherical aggregates is about 5 nm as shown in Fig. 6b. Since the size of nanoparticles is larger than the openings of the clinoptilolite lattice (about 0.4 nm), crystallization of ZnO must occur at the surface of the particles. The SAED pattern recorded over multiple ZnO particles (Fig. 6c) corresponds to the polycrystalline wurtzite ZnO. Comparison between *d*-values measured from the SAED pattern and from the wurtzite ZnO reference is given in Table 4.

**Table 4**
Comparison between measured *d*-values of ZnO nanoparticles from SAED pattern and ZnO reference.

| Distance (nm) | $d_1$ | $d_2$ | $d_3$ |
|---|---|---|---|
| Measured distance (nm) | 0.243 | 0.167 | 0.132 |
| Distance in ZnO (JCPDS 00-003-0888) | 0.246 | 0.161 | 0.130 |
| Crystallographic plane | {1 0 1} | {1 1 0} | {0 0 4} |

### 3.5. Antibacterial activity of Zn-CLI

The results of the antibacterial activity study of the Zn-CLI and ZnO-CLI against *A. junii* are given in Table 5. The activity of Zn-CLI is better than the antibacterial activity of the clinoptilolite which contains nano ZnO particles.

After 24 h of contact with Zn-CLI, a portion of the *A. junii* was immobilized onto the material, while the rest of the bacteria remained as planktonic cells in wastewater. The number of *A. junii* immobilized onto particles of Zn-CLI ($0.39 \times 10^6$ CFU $g^{-1}$) and ZnO-CLI ($61 \times 10^6$ CFU $g^{-1}$) is far lower than the numbers of *A. junii* immobilized onto other zeolite tuffs: $9.5 \times 10^9$ CFU $g^{-1}$ immobilized on Mg-exchanged clinoptilolite [23], $5.3 \times 10^9$ CFU $g^{-1}$ on a surfactant-modified clinoptilolite [24] and $2.3 \times 10^9$ CFU $g^{-1}$ on the natural clinoptilolite [25]. The final number of total cells in the reactor with Zn-CLI and the increase of bacterial numbers (expressed as ratio of the final and starting numbers of bacteria) were significantly lower than in the control reactor. This suggests that Zn-CLI exhibits a strong antibacterial activity to *A. junii*, with a significant (99%) inhibition of bacteria. The final pH values in the reactor with Zn-CLI (pH ~ 6, Table 5) were significantly lower than in the control reactor, but that cannot be regarded as a reason for the decay of bacteria, since this bacterium grows in the pH range 6–8 [26]. That the change of pH is not the reason is confirmed by the results obtained in the reactor with ZnO-CLI where the pH changed only for 0.1 units but the inhibition of bacteria was practically the same as in reactor with Zn-CLI. In spite of the very low number of immobilized bacteria, the P removal in reactors with Zn-CLI was significantly higher than in the control reactor. In separate experiments the P removal by Zn-CLI and ZnO-CLI was tested by incubating a 1.0 g of material in 100 $cm^3$ of synthetic wastewater without the addition of *A. junii*. After 24 h of incubation the reduction of the starting P concentration was 80% and 50% in the reactors with Zn-CLI and ZnO-CLI, respectively. From the difference obtained in experiments using Zn-CLI (or ZnO-CLI) with and without addition of bacteria, it follows that *A. junii* in the reactor with Zn-CLI (ZnO-CLI) removed less than 0.06% of the starting P, thus showing a negligible contribution of bacteria to the P removal. The conclusion is that Zn-CLI and ZnO-CLI by themselves effectively remove phosphate ions from solution.

During the past decade the biological removal of phosphate ions has attracted a great attention [27]. The phosphate biosorption, however, has numerous operational disadvantages [27,28]. Natural zeolites too are unsuitable for the purpose since they show negligible affinity for adsorption of anions; their use as low cost sorbents for the removal of anions, such as phosphate or arsenate, would require a prior modification of the zeolite surface, thus entailing additional costs [24]. However, the results of the present study suggest that the residual Zn-CLI obtained after the removal of Zn from wastewater could find a possible application for a simultaneous phosphate removal and disinfection of wastewater. In that context it is of importance that only a very small amount of Zn(II) can be leached out. The leaching test shows that the resulting Zn(II)

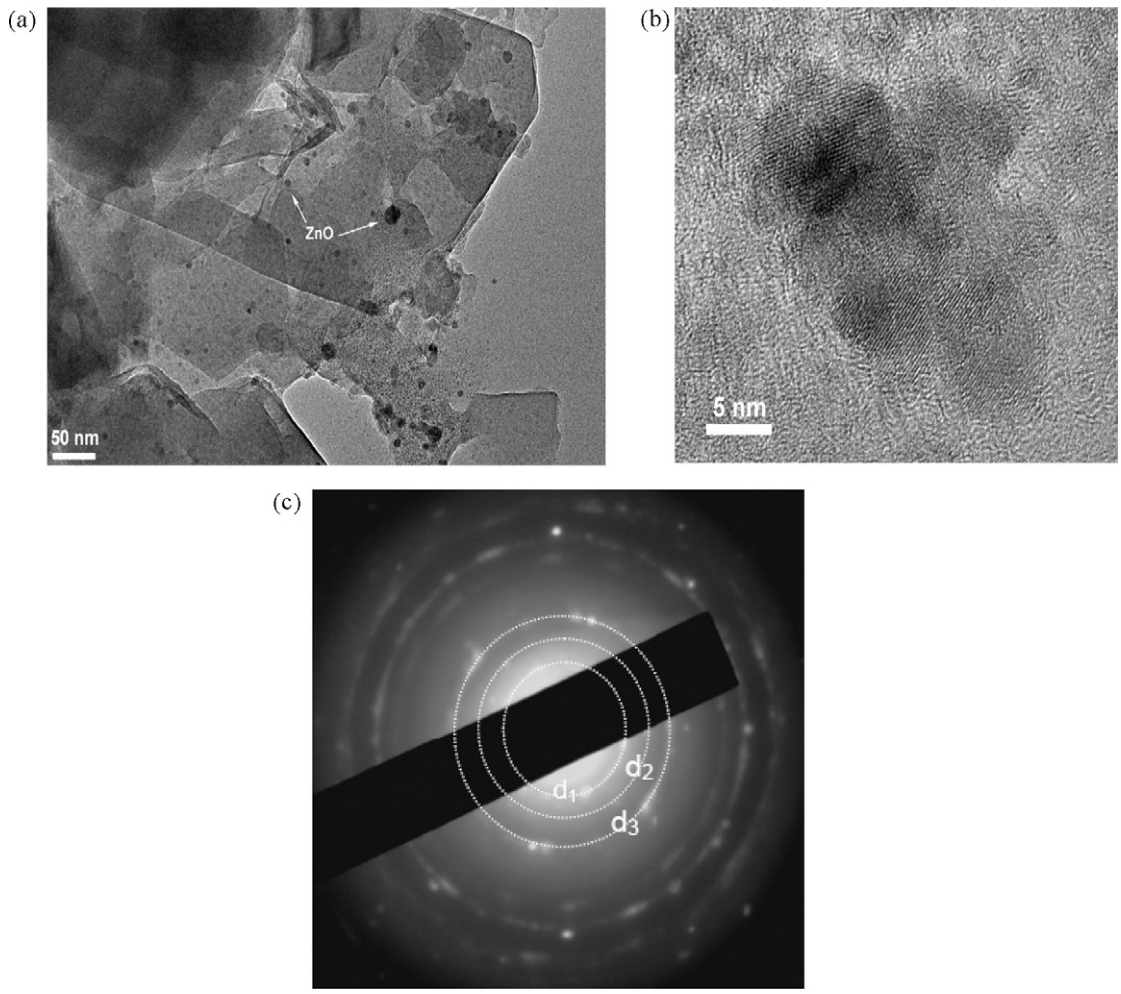


**Fig. 6.** TEM image of the dehydrated Zn-CLI. (a) Hexagonal plates of the clinoptilolite crystals sprinkled with ZnO (dark spots), (b) enlarged view showing nano-sized ZnO (dark area), and (c) the SAED pattern recorded over an area of ZnO particles; diffraction rings can be attributed to the wurtzite ZnO.

**Table 5**
Performance of reactors containing *A. junii* (control), *A. junii* and Zn-CLI, *A. junii* and ZnO-CLI after 24 h of incubation. [$C_0$ CFU ($\times 10^{10}$ dm$^{-3}$)] = 5.33 ± 0.52; [$C_0$(P) (mg dm$^{-3}$)] = 21.05 ± 0.70. Bacteria in reactors with Zn-CLI and ZnO-CLI removed less than 0.06% of the initial P.

| Parameter | Control | ZnO-CLI | Zn-CLI |
|---|---|---|---|
| Final pH | 7.28 ± 0.02 | 7.19 ± 0.02$^{A}$ | 5.99 ± 0.02$^{A,B}$ |
| Immobilized cells ($\times 10^6$ CFU g$^{-1}$) | – | 61.40 ± 2.71 | 0.39 ± 0.02$^{B}$ |
| Planktonic cells ($\times 10^8$ CFU dm$^{-3}$) | 2560.00 ± 636.00 | 3.43 ± 0.06$^{A}$ | 0.016 ± 0.004$^{A,B}$ |
| Total cells ($\times 10^8$ CFU dm$^{-3}$) | 2560.00 ± 636.00 | 3.44 ± 0.06$^{A}$ | 0.016 ± 0.004$^{A,B}$ |
| CFU final/CFU start | 4.85 ± 0.89 | 0.01 ± 0.00$^{A}$ | 0.00 ± 0.00$^{A}$ |
| Inhibition (%) | – | 99.862 ± 0.032 | 99.999 ± 0.000$^{A,B}$ |
| P removed (%) | 38.23 ± 0.53 | 50.12 ± 0.49$^{A}$ | 80.89 ± 0.42$^{A,B}$ |

Significantly different values: $^{A}$compared to control; $^{B}$compared to ZnO-CLI.

concentration in solution is only 0.67 ppm under the experimental conditions.

## 4. Conclusions

The study shows that the Serbian natural zeolite is moderately effective in removing the zinc(II) ions from aqueous solutions by adsorption. At 298 K the sorption capacity varies from 13 to 26% for the initial Zn(II) solution concentration of 100 and 600 mg Zn dm$^{-3}$, respectively; it increases with temperature, so that at 338 K it varies from 18 to 37%.

The sorption isotherm for Zn(II) on clinoptilolite at 298–338 K is best represented by the Langmuir model and the sorption kinetics by the pseudo-second-order model. The sorption involves a combination of three processes: the film diffusion, the intra-particle diffusion, and a chemical cation-exchange between the $Na^+$ ions of clinoptilolite and the $Zn^{2+}$ ions. The sorption was found to be endothermic and spontaneous in the 298–338 K range.

The results concerning antibacterial activity suggest that the exhausted sorbent could find further application since it exhibits an excellent antibacterial activity towards *A. junii*. It also effectively removes phosphate ions from solution. Therefore the Zn-containing clinoptilolite is a promising material in a final step of wastewater treatment, in which a simultaneous phosphate removal and disinfection can be achieved.

Dehydration of Zn-CLI at about 500 °C leads to the formation of wurtzite nano-sized polycrystalline zinc oxide particles which are widespread over clinoptilolite surface. This material also exhibits

disinfecting activity but is less effective in the P removal than Zn-CLI. However, the ZnO nanoclusters incorporated in the zeolitic lattice have been known to exhibit catalytic activity for several reactions [29]. This renders ZnO-CLI a potential candidate for novel applications.

## Acknowledgements

This work was supported by the Serbian Ministry of Science (project no. 142055), Eureka project no E!4208 and the Ministry of Science, Education and Sports of the Republic of Croatia (project no. 1191155-1203). The authors are grateful to Dr. Natasa Zabukovec Logar for the XPS data. The authors also thank the Nemetali Company from Vranjska Banja (Serbia) for kindly providing the zeolite samples.

## References

[1] Š. Cerjan Stefanović, N. Zabukovec Logar, K. Margeta, N. Novak Tušar, I. Arčon, K. Maver, J. Kovač, V. Kaučič, Structural investigation of $Zn^{2+}$ sorption on clinoptilolite tuff from the Vranjska Banja deposit in Serbia, Micropor. Mesopor. Mater. 105 (2007) 251–259.
[2] A. Top, S. Ulku, Silver, zinc, and copper exchange in a Na-clinoptilolite and resulting effect on antibacterial activity, Appl. Clay Sci. 27 (2004) 13–19.
[3] M. Polat, E. Guler, E. Lederman, H. Cohem, Neutralization of an extremely acidic sludge and stabilization of heavy metals in flyash aggregates, Water Manage. 27 (2007) 482–489.
[4] S. Babel, D. del Mundo Dacera, Heavy metal removal from contaminated sludge for land application: a review, Waste Manage. 26. (2006) 988–1004.
[5] N. Rajic, D. Stojakovic, S. Jevtic, S.N. Zabukovec Logar, M. Mazaj, V. Kaucic, Removal of aqueous manganese using the natural zeolitic tuff from the Vranjska Banja deposit in Serbia, J. Hazard. Mater. 172 (2010) 1450–1457.
[6] S. Kocaoba, Y. Orhan, T. Akyüz, Kinetics and equilibrium studies of heavy metal ions removal by use of natural zeolite, Desalination 214 (2007) 1–10.
[7] N. Rajic, Dj. Stojakovic, A. Recnik, Thermal deamination kinetics of the nickel-containing chabazite-like aluminophosphate, $Ni(NH_2\text{-}CH_2\text{-}CH_2\text{-}NH_2)(2)(AlPO_4)(6)(OH)(2)$, deposition of nanocrystalline NiO particles, Inorg. Chim. Acta 362 (2009) 5139–5143.
[8] L.E. de Bashan, Y. Bashan, Recent advances in removing phosphorus from wastewater and its future use as fertilizer (1997–2003), Water Res. 38 (2004) 4222–4246.
[9] D.R. Durham, L.C. Marshall, J.G. Miller, A.B. Chmurny, Characterization of inorganic biocarriers that moderate system upsets during fixed-film biotreatment process, Appl. Environ. Microbiol. 60 (1994) 3329–3335.
[10] K. Vijayaraghavan, Y. Yun, Bacterial biosorbents and biosorption, Biotechnol. Adv. 26 (2008) 266–291.
[11] Y.S. Ho, J.F. Porter, G. McKay, Equilibrium isotherm studies for the sorption of divalent metal ions onto peat: copper, nickel and lead single component systems, Water Air Soil Pollut. 141 (2002) 1–33.
[12] M.A. Stylianou, M.P. Hadjiconstantinou, V.J. Inglezakis, K.G. Moustakas, M.D. Loizidou, Use of natural clinoptilolite for the removal of lead, copper and zinc in fixed bed column, J. Hazard. Mater. 143 (2007) 575–581.
[13] N. Gupta, S.S. Amritphale, N. Chandra, Removal of Zn(II) from aqueous solution by using hybrid precursor of silicon and carbon, Bioresour. Technol. 101 (2010) 3355–3362.
[14] B. Alyuz, S. Veli, Kinetics and equilibrium studies for the removal of nickel and zinc from aqueous solutions by ion exchange resins, J. Hazard. Mater. 167 (2009) 482–488.
[15] M. Arshad, M.N. Zafar, S. Younis, R. Nadeem, The use of Neem biomass for the biosorption of zinc from aqueous solutions, J. Hazard. Mater. 157 (2008) 534–540.
[16] Y. Ho, Review of second-order models for adsorption systems, J. Hazard. Mater. B136 (2006) 681–689.
[17] M. Rafatullah, O. Sulaiman, R. Hashim, A. Ahmad, Adsorption of copper(II), chromium(III), nickel(II) and lead(II) ions from aqueous solution by meranti sawdust, J. Hazard. Mater. 170 (2009) 969–977.
[18] T.-C. Hsu, Experimental assessment of adsorption of $Cu^{2+}$ and $Ni^{2+}$ from aqueous solution by oyster shell powder, J. Hazard. Mater. 171 (2009) 995–1000.
[19] W.J. Weber Jr., J.C. Morris, Kinetics of adsorption on carbon from solution, J. Sanit. Eng. Div. Am. Soc. Civ. Eng. 89 (1963) 31–60.
[20] W.H. Cheung, Y.S. Szeto, G. McKay, Intraparticle diffusion processes during acid dye adsorption onto chitosan, Bioresour. Technol. 98 (2007) 2897–2904.
[21] R. Aravindhan, J. Raghava Rao, B. Unni Nair, Preparation and characterization of activated carbon from marine macro–algal biomass, J. Hazard. Mater. 162 (2009) 688–694.
[22] D. Nibou, H. Mekatel, S. Amokrane, M. Barkat, M. Trari, Adsorption of $Zn^{2+}$ ions onto NaA and NaX zeolites: kinetic, equilibrium and thermodynamic studies, J. Hazard. Mater. 173 (2010) 637–646.
[23] J. Hrenovic, T. Ivankovic, D. Tibljas, The effect of mineral carrier composition on phosphate-accumulating bacteria immobilization, J. Hazard. Mater. 166 (2009) 1377–1382.
[24] J. Hrenovic, M. Rozic, L. Sekovanic, A. Vucinic-Anic, Interaction of surfactant-modified zeolites and phosphate accumulating bacteria, J. Hazard. Mater. 156 (2008) 576–582.
[25] J. Hrenovic, D. Tibljas, Y. Orhan, H. Buyukgungor, Immobilisation of *Acinetobacter calcoaceticus* using natural carriers, Water SA 31 (2005) 261–266.
[26] G.M. Garrity, D.J. Brenner, N.R. Krieg, J.T. Staley, Bergey's Manual of Systematic Bacteriology, vol. 2, Part B, Springer, New York, 2005.
[27] Y. Liu, T. Zhang, H.H.P. Fang, Microbial community analysis and performance of a phosphate-removing activated sludge, Bioresour. Technol. 96 (2005) 1205–1214.
[28] U. Farooq, J.A. Kozinski, M.A. Khan, M. Athar, Biosorption of heavy metal ions using wheat based biosorbents—a review, Bioresour. Technol. 101 (2010) 5043–5053.
[29] R. Anand, T.M. Jyothi, B.S. Rao, A comparative study on the catalytic activity of ZnO modified zeolites in the synthesis of alkylpyrazines, Appl. Catal. A 208 (2001) 203–211.